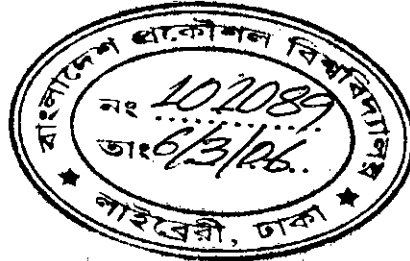
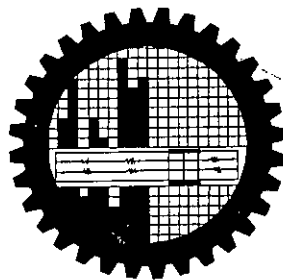


**A new technique for determining Base Transit Time of a BJT
considering field dependent mobility**



A thesis submitted to the Department of Electrical and Electronic Engineering (EEE)
of
Bangladesh University of Engineering and Technology (BUET)
in partial fulfillment of the requirement for the degree of
MASTER OF SCIENCE IN ELECTRICAL AND ELECTRONIC ENGINEERING

by
Md. Waliullah Khan Nomani

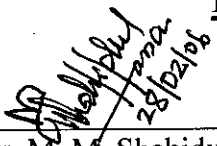

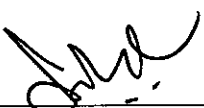
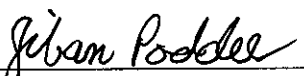


**DEPARTMENT OF ELECTRICAL AND ELECTRONIC ENGINEERING (EEE)
BANGLADESH UNIVERSITY OF ENGINEERING AND TECHNOLOGY
(BUET)
2006**



The thesis titled “A new technique for determining Base Transit Time of a BJT considering field dependent mobility” submitted by Md. Waliullah Khan Nomani, Roll No.: 040406240P, Session: April 2004 has been accepted as satisfactory in partial fulfillment of the requirement for the degree of MASTER OF SCIENCE IN ELECTRICAL AND ELECTRONIC ENGINEERING on February 28, 2006.

BOARD OF EXAMINERS

1. 
Dr. M. M. Shahidul Hassan
Professor
Department of Electrical and Electronic Engineering
BUET, Dhaka—1000, Bangladesh.
Chairman
(Supervisor)
2. 
Dr. S. Shahnawaz Ahmed
Professor & Head
Department of Electrical and Electronic Engineering
BUET, Dhaka—1000, Bangladesh.
Member
(Ex-officio)
3. 
Dr. Quazi Deen Mohd Khosru
Professor
Department of Electrical and Electronic Engineering
BUET, Dhaka—1000, Bangladesh.
Member
4. 
Dr. Jiban Podder
Professor
Department of Physics
BUET, Dhaka—1000, Bangladesh.
Member
(External)

DECLARATION

I hereby declare that this thesis or any part of it has not been submitted elsewhere for the award of any degree or diploma.

Signature of candidate

Waliullah
08.03.06

(Md. Waliullah Khan Nomani)

DEDICATION

To My Parents

TABLE OF CONTENTS

Declaration	iii
Dedication	iv
List of Figures	vii
List of Symbols	ix
Acknowledgement	xi
Abstract	xii
1. Introduction	1
1.1 Bipolar Junction Transistor	1
1.2 Base Transit Time	3
1.3 Reviews of Recent Works on Base Transit Time	3
1.4 Objective of the Thesis	5
1.5 Summary of the Thesis	5
2. Mathematical Analysis	6
2.1 Introduction	6
2.2 Derivation of the Model Equations	6
2.2.1 Model Equations For Low Injection	8
2.2.2 Model Equations For High Injection	12
2.4 Conclusion	16
3. Results & Discussion	17
3.1 Introduction	17
3.2 Results and Discussions	17
3.2.1 Distribution of Minority Carrier within the Base	17

3.2.2 Electric Field Distribution within the Base	20
3.2.3 Variation of Collector current density with Base-emitter voltage	22
3.2.4 Variation of Base Transit Time with Minority Carrier Injection Ratio	24
3.2.5 Variation of Base Transit Time with Base-Emitter Voltage	26
3.2.6 Dependence of Base Transit Time upon Base Width	26
3.2.7 Dependence of Base Transit Time upon Peak Base Doping Concentration	28
3.2.8 Dependence of base transit time upon field dependent mobility	29
3.2.9 Dependence of base transit time upon slope of base doping	30
3.3 Conclusion	31
4. Conclusion and Suggestions	32
4.1 Conclusion	32
4.2 Suggestions for Future Works	32
References	33

LIST OF FIGURES

Fig. 1.1 An n^+ -p-n bipolar junction transistor.	2
Fig. 2.1 Minority carrier density profile in the base obtained from the model for low level of injection and numerical solution for high level of injection.	12
Fig. 3.1(a) Injected minority carrier distribution within the base for two different peak base doping.	18
Fig. 3.1(b) Normalized injected electron concentration profile for various base widths.	18
Fig. 3.1(c) Injected minority carrier distribution within the base for various slope of base doping profile.	19
Fig. 3.1(d) Minority carrier injection ratio as a function of base-emitter voltage.	19
Fig. 3.2(a) Electric field distribution with in the base for two different peak base doping concentrations. Solid line represents high injection (for $V_{be} = 0.85V$) and dotted line represents low injection (for $V_{be} = 0.7V$).	21
Fig 3.2(b) Electric field distribution with in the base for two different slope of base doping concentrations. Solid line represents high injection (For $V_{be} = 0.85V$) and dotted line represents low injection (for $V_{be} = 0.7V$)	22
Fig. 3.3(a) Collector current density as a function of base-emitter voltage For two different peak base doping concentrations.	23
Fig. 3.3(b) Collector current density as a function of base-emitter voltage For two different slope of exponentially doped base.	23

Fig. 3.3(c) Comparison of analytically calculated electron current density With the numeric electron current density [7] as a function of base-emitter voltage.	24
Fig. 3.4(a) Base transit time as a function of minority carrier injection ratio For three different base peak doping concentrations.	25
Fig. 3.4(b) Comparison of base transit time as a function of minority Carrier injection ratio calculated from the present model With the numerical result [7].	25
Fig 3.5 Base transit time as a function of base-emitter voltage for three different peak base doping concentrations.	26
Fig 3.6(i) Base transit time as a function of base width.	27
Fig 3.6(ii) Base transit time as a function of base width. The circle represents base transit time for [20] and the line represents the present model.	28
Fig. 3.7 Dependence of base transit time on peak base doping concentration as a function of base-emitter voltage	29
Fig. 3.8 Base transit time as a function of base-emitter voltage with and without considering field dependence of mobility.	30
Fig. 3.9 Base transit time as a function of slope of base doping profile.	31

LIST OF SYMBOLS

Symbols	Description
D_n	Diffusion co-efficient for electron
μ_n	Electron mobility in the base
E	Electric field
E_c	Critical electric field
f_T	Cut-off frequency
f_{\max}	Maximum frequency of operation
J_n	Electron current density for all levels of injection
J_{nl}	Current density for low injection region
J_{nl2}	Current density for low injection region considering Webster effect
J_c	Collector current density
I_E	Emitter current
n_{ie}	Effective intrinsic carrier concentration
$p(x)$	Hole concentration in the base
$n(x)$	Injected carrier concentration for high injection
$n_l(x)$	Injected carrier concentration for low injection
$n_{l2}(x)$	Injected carrier concentration for low injection considering Webster effect
$\delta n(x)$	Change in injected electron concentration at high injection from low injection

n_{i0}	Intrinsic carrier concentration without any bandgap narrowing
$N_A(0)$	Base peak doping concentration in the base
Q_{lb}	Stored base charge per unit area for low injection
Q_b	Stored base charge density for all levels of injection
W_b	Base width
v_s	Saturation velocity
k	Boltzmann constant
T	Absolute temperature
η	Slope of base doping
γ_1	0.42
γ_2	0.69
τ_{lb}	Base transit time for low injection
τ_b	Base transit time for all levels of injection

ACKNOWLEDGEMENT

I wish to convey my heartiest gratitude and profound respect to my supervisor Dr. M. M. Shahidul Hassan, Professor Department of Electrical and Electronic Engineering (EEE), Bangladesh University of Engineering and Technology (BUET), Dhaka, Bangladesh, for his continuous guidance, suggestion and wholehearted supervision throughout the progress of this work, without which this thesis never be materialized. I am grateful to him for acquainting me with the world of advanced research. I am also grateful to him for providing the computing facilities.

I like to thank the present Head and Professor of the Department of Electrical and Electronic Engineering, BUET, Dr. S. Shahnawaz Ahmed for providing me the lab facilities.

I want to thank Mr. Md. Ziaur Rahman Khan, Mr. Touhidur Rahman and other colleagues, who were directly or indirectly related to this work, for their support and encouragement. I also thank all the personnel of the departmental library, BUET reference library and Xerox section for providing me with the valuable journals and thesis papers to complete this work.

I am grateful to all the member of my family especially to my father, mother and elder brother for their cooperation and support throughout the entire period of this work.

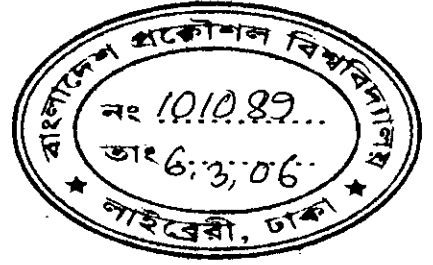
Finally I am grateful to Almighty Allah for giving me the strength and courage to complete this thesis.

ABSTRACT

A base transit time model for an *npn* bipolar junction transistor with exponential-doped base at high level of injection, which is applicable for all levels of injection before the onset of the Kirk effect, is developed. Based on the realistic assumption that a small change in electron concentration in the base at high injection occurs from its modified low injection model incorporating Webster effect, mathematical expressions for minority carrier concentration and current density have been derived. In this work, electric field dependence of mobility in addition to doping dependent mobility, bandgap-narrowing effect, high-injection effect and carrier velocity saturation at the base edge of the base-collector junction are incorporated. The base transit time is found to be different if the field dependent mobility is considered. The study shows that the base transit time depends on base-emitter voltage, minority carrier injection ratio, peak base doping density, slope of base doping profile and base width. The analytically calculated base transit time is found to be in good agreement with numerical results available in literature.

CHAPTER ONE

INTRODUCTION



1.1 BIPOLAR JUNCTION TRANSISTOR

The bipolar junction transistor (BJT), one of the most important semiconductor devices, was invented by a research team at Bell Laboratories in 1947. It has had an unprecedented impact on the electronic industry in general and on solid-state research in particular. Before 1947 semiconductors were only used as thermistors, photodiodes, and rectifiers. In 1948 John Bardeen and Walter Brattain announced the development of the point-contact transistor [1]. In the following year William Shockley's classic paper on junction diode and transistors was published [2]. Their work at Bell Laboratories was highly successful, which led them to the bipolar junction transistor. They used germanium as the semiconductor of choice because it was possible to obtain high purity material. The extraordinarily large diffusion length of minority carriers in germanium provided functional structures despite the large dimensions of the early devices. Since then, the technology has progressed rapidly. The development of a planar process yielded the first circuits on a chip and for a decade, bipolar transistor operational amplifiers, like the 741, and digital TTL circuits were for a long time the workhorses of any circuit designer. During the last decade spectacular rise of the MOSFET has occurred. Almost all logic circuits, microprocessors and memory chips contain exclusively MOSFETs. Nevertheless, bipolar transistors remain important devices for ultra-high-speed discrete logic circuits such as emitter coupled logic (ECL), in vehicles and satellites, in power-switching applications and in microwave power amplifiers. Heterojunction bipolar transistors (HBTs) have emerged as the device of choice for cell phone amplifiers and other demanding applications.

A bipolar junction transistor consists of two back-to-back p-n junctions, who share a thin common region with width, W_b . When the common region is doped with acceptor atoms and the other two regions are doped with donor atoms the transistor is called an

n-p-n bipolar junction transistor. For opposite types of doping in these regions, the transistor becomes a p-n-p bipolar junction transistor. Contacts are made to all three regions, the two outer regions are called the emitter and the collector and the middle region is called the base. For practical interest, doping concentration of emitter is made very high. Thus it forms an n⁺-p-n structure.

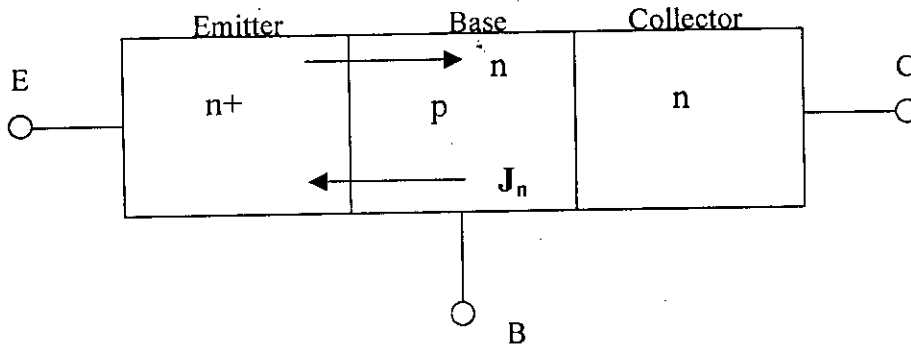


Fig. 1. An n⁺-p-n bipolar junction transistor.

For a good n⁺-p-n transistor, we expect that almost all the electrons injected by the emitter into the base be collected in the collector. So the p-type base region should be thin. This requirement is summed up by specifying neutral base width should be less than the diffusion length of electron in the base. With this requirement satisfied, an average electron injected at the emitter junction will diffuse to the depletion region of the base-collector junction without recombination in the base. A second requirement is that the emitter current, I_E crossing the emitter junction should be composed almost entirely of electrons injected into the base, rather than holes crossing from base to emitter [3]. In our analysis we consider only the forward active bias mode of operation, obtained by forward biasing the base-emitter junction and reverse biasing the base-collector junction.

One of the important figures of merit of BJTs is the cut-off frequency, f_T . Bipolar transistors have been used mainly due to their speed advantage and driving capability. Major applications today are RF front-end as well as fiber-optic circuits, in which the transistors are operated at high frequency. Among different delay terms, the base transit time τ_b is one of the dominant factors in deciding $f_T(1/2\pi\tau)$, where τ is the total delay time. Therefore it is of great importance to obtain an accurate, yet relatively simple analytical model of base transit time and collector current density for high frequency bipolar transistors for efficient device design.

1.2 BASE TRANSIT TIME

The average time taken by minority carriers to diffuse across the quasi-neutral base or the average time that an electron spends in the base is called the base transit time, τ_b . The base transit time depends upon many factors such as base width, base resistance, various concentration profiles in the base region (uniform, linear, exponential and Gaussian), velocity saturation effect, collector current density, quasi-saturation, built-in electric field in the base region, mobility and bandgap-narrowing etc.

The base transit time can be written as [3]

$$\tau_b = \int_0^{W_b} \frac{qn(x)}{J_n(x)} dx \quad (1.1)$$

If the recombination within the base is neglected then electron current within the base is constant and eqn. (1.1) can be written as

$$\tau_b = \frac{1}{J_n} \int_0^{W_b} qn(x) dx = \frac{Q_n}{J_n} \quad (1.2)$$

where, J_n is the current density.

$$\text{and} \quad Q_n = q \int_0^{W_b} n(x) dx \quad (1.3)$$

where, Q_n is the stored base charge per unit area and $n(x)$ is the minority carrier distribution within the base. The base transit time is very important in determining different performance parameter like the maximum frequency of operation (f_{\max}), cut-off frequency (f_T) and the noise figure of a bipolar transistor.

1.3 REVIEW OF RECENT WORKS ON BASE TRANSIT TIME

Bipolar junction transistors (BJTs) have been used mainly due to their speed advantage and driving capability [3]. Therefore, it is of great importance to obtain an accurate, yet relatively simple analytical model of base transit time τ_b and collector current density J_c of modern bipolar transistors for efficient device design. Numerous papers regarding base transit time of BJT have been published [4]-[12]. Analytical models for high level of injection within base have been obtained assuming that the injected electron

concentration $n(x)$ is much larger than the base doping concentration $N_A(x)$ over the entire base region (the strong-high injection model) [13]. Kirk phenomenon [14] will occur at strong-high injection but the Kirk effect was not considered in the models. Therefore, the strong-high injection models are inaccurate. The transit time considering all the effects was determined in the work [7]. The method was based on iterative techniques. So the equation forms for electron current density $J_n(x)$ and base transit time τ_b are not concise and they are inconvenient for us to understand device physics. The iterative method [7] is time-consuming, which calls for further improvement. Suzuki [8] obtained an expression for τ_b for high level of injection using a perturbation theory before the onset of the Kirk effect. But the equation form for τ_b was not concise and included several integrals. Later a set of initial conditions was proposed [10] based on the uniform doping profiles in order to reduce the computational time. As the work [10] is based on iterative technique, it is still not convenient. Using best curve fitting technique, recently few models for base transit time [11, 12] have been derived for high level of injection. In obtaining $n(x)$ and $J_n(x)$ for high level of injection, analytically obtained models for $n(x)$ and $J_n(x)$ for low and strong-high injections have been used. An empirical expression for high level of injection where $n(x)$ is comparable to base doping profile $N_A(x)$ was obtained studying the realistic behaviors of current and charge in case of low and strong high levels of injection. The model for strong high injection was derived assuming that the injected electron concentration is much larger than the base doping concentration over the entire base region. At the high-injection the phenomenon known as Kirk effect will occur. When the Kirk effect occurs the base transit time will become large and will increase with J_C . For this Kirk effect the high injection model is inaccurate. So the empirical expression, which is formulated using the equations, derived for low and strong high levels of injection turns inaccurate.

In this thesis, the analytical models for $n_l(x)$ and $J_{nl}(x)$ at low injection are extended to cover high-level of injection. In addition to doping dependence of mobility, its field dependence is also considered in the present work. In obtaining the analytical form for minority carrier electron current density $J_n(x)$, it is common practice to consider only the doping dependence of mobility. The base transit time is found to be different if field

dependence of mobility is considered. The validity of the assumptions made in obtaining analytical expressions for τ_b and $J_n(x)$ has been verified through numerical results available in literature.

1.4 OBJECTIVE OF THE THESIS

The main objective of this research is to find a mathematical expression for base transit time of an exponentially doped *n*p*n* bipolar junction transistor at high injection by using a new technique. In obtaining minority carrier profile, electric field dependence of mobility in addition to doping dependence of mobility, bandgap narrowing effect, high-injection effect, carrier velocity saturation will be considered. The injected minority carrier, collector current density, stored base charge, electric field in the base and dependence of base transit time on different device parameters will also be studied. It is expected that the derived model will give quick and accurate base transit time for realistic transistors.

1.5 SUMMARY OF THE THESIS

In this work expressions for injected minority carrier concentration profile, collector current density and hence the base transit time of a bipolar junction transistor are derived. In chapter one previous works on base transit time have been reviewed. Mathematical analyses are given in chapter two. In chapter three the dependence of current and transit time on various device parameters are studied. The transit time obtained from the derived equation is compared to that of numerical analysis in order to demonstrate the validity of the assumptions made in deriving expression for base transit time. This paper ends in chapter four containing salient features of this work and possible future field of studies.

CHAPTER TWO

MATHEMATICAL ANALYSIS

2.1 INTRODUCTION

The injected minority carrier concentration profile and collector current density for an *npn* bipolar junction transistor with exponential base doping profile is modeled and calculated for high level of injection. In obtaining minority carrier profile, electric field dependence of mobility in addition to doping dependence of mobility, bandgap-narrowing effect, high-injection effect and carrier velocity saturation at the base edge of the base-collector junction is considered. The derivation of the model equations starts by first considering low level of minority carrier injection within the base. In the proposed new technique the minority carrier profile of low level of injection is extended for finding minority carrier profile for high level of injection by using Webster effect [15]. A minority carrier profile for low level of injection is obtained by solving current continuity equations for holes and electrons, electric field equation, expression for field and doping dependent mobility and intrinsic carrier concentration for high base doping. We assume that for high level of injection $n(x)$, the injected electron concentration is perturbed by the electric field from the modified low injection profile only a small amount $\delta n(x)$. Next we obtain a second order differential equation for $n(x)$ using current continuity equations, electric field equation, expression for field and doping dependent mobility and intrinsic carrier concentration for high base doping again. The solution of this differential equation gives the minority carrier profile of $n(x)$. Once $n(x)$ is known, it is easier to find analytical expressions for J_n , Q_b and τ_b .

2.2 DERIVATION OF THE MODEL EQUATIONS

The electron current density $J_n(x)$ for an arbitrary base doping concentration $N_A(x)$ is given by [16]

$$-J_n = q D_n(x) \frac{dn(x)}{dx} + q \mu_n(x) E(x) n(x) \quad (2.1)$$

and the electric field $E(x)$ is given by

$$E(x) = \frac{kT}{q} \left(\frac{1}{p(x)} \frac{dp(x)}{dx} - \frac{1}{n_{ie}^2(x)} \frac{dn_{ie}^2(x)}{dx} \right) \quad (2.2)$$

where D_n is the diffusion coefficient for electron, μ_n is the mobility for electron, n_{ie} is the effective intrinsic carrier concentration, p is the hole concentration and q is the charge of electron. We define the direction of $J_n(x)$ in (2.1) so that it has a positive value. In obtaining (2.2) the carrier recombination in the base region is neglected. If recombination is neglected, then the collector current density J_c will be equal to J_n . In today's bipolar transistor, carrier recombination in the base is negligible [9], which makes J_n constant.

Substituting (2.2) into (2.1), the current density equation becomes

$$-J_n = q D_n(x) \frac{n_{ie}^2(x)}{n(x) + N_A(x)} \frac{d}{dx} \left[\frac{n(x)[n(x) + N_A(x)]}{n_{ie}^2(x)} \right] \quad (2.3)$$

The effective intrinsic carrier concentration is [17]

$$n_{ie}^2(x) = n_{io}^2 \left(\frac{N_A(x)}{N_r} \right)^{\gamma_2} \quad (2.4)$$

where $n_{io} (= 1.4 \times 10^{10} \text{ cm}^{-3})$ is the intrinsic carrier concentration without any bandgap-narrowing. From (2.1) and (2.2) we can write

$$E(x) = \frac{V_T}{2n(x) + N_A(x)} \left(\frac{dN_A(x)}{dx} - \frac{n(x) + N_A(x)}{n_{ie}^2(x)} \frac{dn_{ie}^2(x)}{dx} - \frac{J_n}{D_n(x)} \right) \quad (2.5)$$

The electric-field dependent mobility is given by an empirical relation [18]

$$\mu_n = \frac{v_s}{\left(1 - \frac{1}{\alpha} \right) E + E_c} \quad (2.6)$$

where $E_c \left(= \frac{v_s}{\mu_{no}} \right)$ is the critical electric field and μ_{no} is the low-field doping density

dependent electron mobility which is given by [17]

$$\mu_{no} = \mu_n(o) \left(\frac{N_A}{N_r} \right)^{-\gamma_1} \quad (2.7)$$

where $\mu_n(o) = 20.72 \text{ cm}^2 (\text{V.s})^{-1}$, $\alpha = 4.43$, $N_r = 10^{17} \text{ cm}^{-3}$, $n_{i0} = 1.4 \times 10^{10} \text{ cm}^{-3}$, $\gamma_1 = 0.42$ and $\gamma_2 = 0.69$.

The derivation of the model equations starts by first considering low level of minority carrier injection within the base. The expressions for Q_b and J_n are obtained for low injection. For high injection where $n(x)$ is comparable to $N_A(x)$, (2.3) is not analytically tractable. We have extended the low-injection model. General formulation for J_n and Q_b is obtained by making a realistic assumption that the injected electron concentration $n(x)$ at high injection is perturbed by modulated electric field from its modified low concentration $n_{l2}(x)$ (see (2.25)) only a little amount $\delta n(x)$ (see section 2.2.2).

2.2.1 Model Equations For Low Injection

For low injection, $n_l(x) \ll N_A(x)$ and the quasi-neutral condition becomes

$$N_A(x) + n_l(x) \approx N_A(x) \quad (2.8)$$

In this work the base is assumed to be exponentially doped and doping is given by [19]

$$N_A(x) = N_A(0) e^{-\frac{\eta x}{W_b}} \quad (2.9)$$

where $N_A(0)$ is the peak base doping concentration and η is the slope of base doping profile. The slope η can be expressed as

$$\eta = \ell n \left(\frac{N_A(0)}{N_A(W_b)} \right) \quad (2.10)$$

where $N_A(W_b)$ is the doping density at $x = W_b$.

Using (2.2), (2.4), (2.8) and (2.9) electric field can be expressed as

$$E = -\frac{\eta V_T}{W_b} (1 - \gamma_2) \quad (2.11)$$

Using (2.1), (2.4), (2.6) and (2.11) we can write

$$\frac{dn_l(x)}{dx} - \frac{\eta}{W_b} (1 - \gamma_2) n_l(x) = -\frac{J_{nl}}{q V_T \mu_n(o)} \left(\frac{N_A(0)}{N_r} \right)^{\gamma_1} e^{-\frac{\eta \gamma_1}{W_b} x} + \frac{\alpha \eta J_{nl}}{q v_s W_b} (1 - \gamma_2) \quad (2.12)$$

where

$$a = \left(1 - \frac{1}{\alpha}\right)$$

The solution of (2.12) is

$$n_l(x) = n_l(0) e^{-\frac{\eta(1-\gamma_2)}{W_b}x} + \frac{FW_b}{\eta(1+\gamma_1-\gamma_2)} \left(e^{-\frac{\eta\gamma_1}{W_b}x} - e^{-\frac{\eta(1-\gamma_2)}{W_b}x} \right) + \frac{aJ_{nl}}{qv_s} \left(1 - e^{-\frac{\eta(1-\gamma_2)}{W_b}x} \right) \quad (2.13)$$

where $n_l(0)$ is the electron density at $x = 0$

and

$$F = \frac{J_{nl}}{qD_n(0)} \left(\frac{N_A(0)}{N_r} \right)^{\gamma_1}$$

Assuming that the electron velocity in the base-collector depletion region saturates at v_s , the electron current density J_{nl} at $x = W_b$ is given by

$$J_{nl} = qv_s n_l(W_b) \quad (2.14)$$

Using (2.14) in (2.13), and putting $x = W_b$ electron concentration $n_l(W_b)$ can be written as

$$n_l(W_b) = \frac{n_l(0)e^{\eta(1-\gamma_2)}}{1 + a \left(e^{\eta(1-\gamma_2)} - 1 \right) + \frac{v_s W_b}{\eta D_n(0)(1+\gamma_1-\gamma_2)} B_d} \quad (2.15)$$

where

$$B_d = \left(\frac{N_A(0)}{N_r} \right)^{\gamma_1} \left(e^{\eta(1-\gamma_2)} - e^{-\eta\gamma_1} \right)$$

For a base with uniformly doped concentration N_A , $n_l(W_b)$ can be obtained by substituting $\eta = 0$ in (2.15) and is found to be of the form

$$n_l(W_b) = \frac{n_l(0)}{1 + \frac{v_s W_b}{D_n(0)} \left(\frac{N_A}{N_r} \right)^{\gamma_1}} \quad (2.16)$$

Substituting the value of $n_l(W_b)$ from (2.15) in (2.14) and rearranging it, J_{nl} for low injection can be expressed as $J_{nl} = A_{low} n_{l0}$ (2.17)

Where $n_{lo} = \frac{n_I(0)}{N_A(0)}$ is the normalized carrier concentration for low injection and

$$A_{low} = \frac{N_A(0)e^{\eta(1-\gamma_2)}}{1 + a\left(e^{\eta(1-\gamma_2)} - 1\right) + \frac{v_s W_b}{\eta D_n(0)(1+\gamma_1-\gamma_2)} B_d}$$

The base stored charge per unit area for low injection

$$Q_{lb} = \int_0^{W_b} n_I(x) dx = qB_{low}n_{lo} \quad (2.18)$$

where

$$B_{low} = A_{low} \left(-\frac{W_b^2 (e^{-\eta\gamma_1} - 1)}{qD_n(0)\eta^2\gamma_1(1+\gamma_1-\gamma_2)} \left(\frac{N_A(0)}{N_r}\right)^{\gamma_1} + \frac{aW_b}{qv_s} - \frac{W_b (e^{\eta(1-\gamma_2)} - 1)}{q\eta(1-\gamma_2)} B_{I1} \right)$$

and

$$B_{I1} = \frac{W_b}{D_n(0)\eta(1+\gamma_1-\gamma_2)} \left(\frac{N_A(0)}{N_r}\right)^{\gamma_1} + \frac{a}{v_s} - \frac{qN_A(0)}{A_{low}}$$

For uniformly doped base, Q_{lb} from (2.18) can be obtained as

$$Q_{lb} = -\frac{W_b^2}{2D_n} n_I(W_b)qv_s + qn_I(0)W_b \quad (2.19)$$

The base transit time for low injection for exponentially doped base can be obtained from (2.17) and (2.18) and can be written as

$$\tau_{lb} = q \frac{B_{low}}{A_{low}} \quad (2.20)$$

Using (2.14), (2.16) and (2.19) the base transit time for uniformly doped base can be expressed as

$$\tau_{lb} = \frac{W_b^2}{2D_n} + \frac{W_b}{v_s} \quad (2.21)$$

where

$$D_n = D_n(0) \left(\frac{N_A}{N_r}\right)^{-\gamma_1}$$

Base transit time in (2.21) is exactly similar to the expression for τ_b derived in [9] for low level of injection for uniformly doped base.

2.2.2 Model Equations For High Injection

It has been found that the injected electron concentration at high injection $n(x)$ is not significantly changed from $n_I(x) f_w$ for a box-doped base [17]. We, therefore, expect that the result is also valid for arbitrarily doped bases. For justification of this assumption at high level of injection, we have numerically obtained the injected minority carrier electron concentration profile $n(x)$ at high injection for an exponentially doped base for two different peak base doping profile. In obtaining numeric solution of injected electron density profile, differential equation (2.1) and (2.5) were normalized and solved by ODE routines in the MATLAB. For a given value of the base-emitter junction voltage V_{be} , the initial value of $n(0)$ and J_n were required. The initial value $n(0)$ was obtained from the following relation [13, 15]

$$n(0) = \frac{n_{ie}^2}{N_A(0)} \exp\left(\frac{qV_{be}}{kT}\right) f_w \quad (2.22)$$

where

$$f_w = \frac{1}{\frac{1}{2} + \sqrt{\frac{1}{4} + \frac{n_{ie}^2}{N_A^2} e^{\left(\frac{qV_{be}}{kT}\right)}}} \quad (2.23)$$

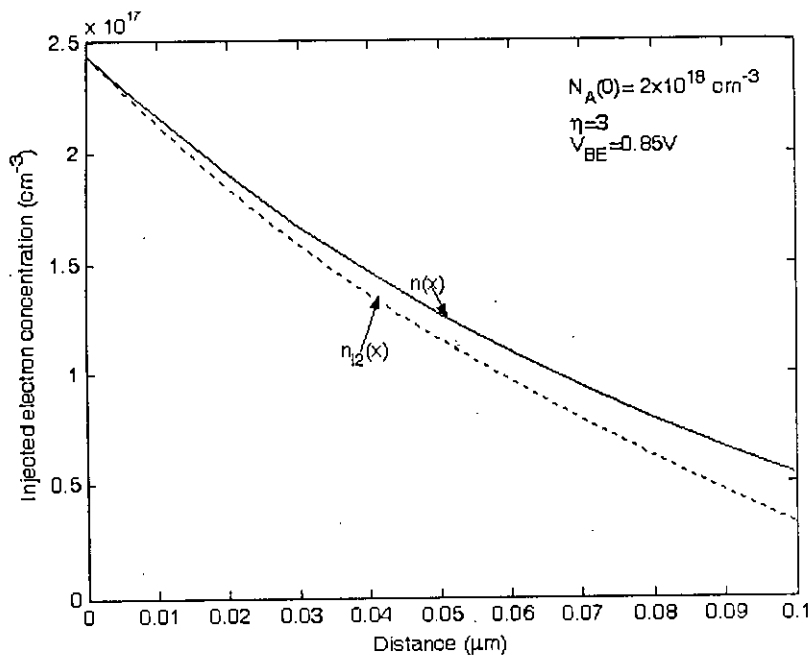
First a trial value of J_n was chosen and the solution was obtained when the trial value was found equal to the value $qv_s n_{I2}(W_b)$. Numerically obtained $n(x)$ for exponentially doped base is also found not significantly different from $n_{I2}(x)$ (Fig. 1). Considering the Webster effect [15] we can write

$$n_{I2}(x) = n_I(x) f_w \quad (2.24a)$$

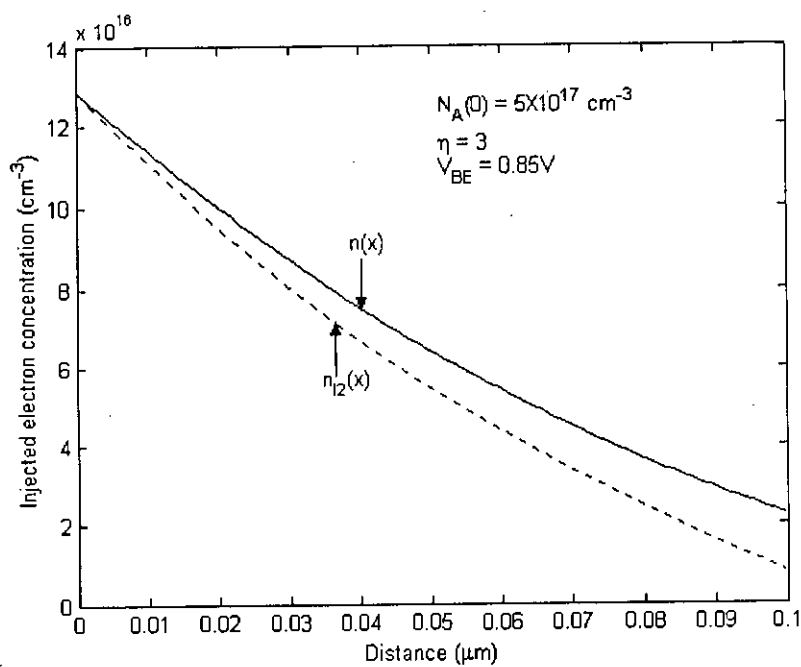
$$J_{nI2}(x) = J_{nI}(x) f_w \quad (2.24b)$$

Assume that $n(x)$ is perturbed by the modulated electric field from $n_{I2}(x)$ only a little, that is

$$n(x) = n_{I2}(x) + \delta n(x) \quad (2.25)$$



(a)



(b)

Fig. 2.1 Minority carrier density profile in the base obtained from the model for low level of injection and numerical solution for high level of injection.

Substituting (2.25) in (2.1) and (2.2), we obtain a linear first order differential equation for $n(x)$

$$-J_n = q D_n(x) \frac{n_{ie}^2(x)}{n_{l2}(x) + \delta n(x) + N_A(x)} \frac{d}{dx} \left[\frac{[n_{l2}(x) + \delta n(x)][n_{l2}(x) + \delta n(x) + N_A(x)]}{n_{ie}^2(x)} \right] \quad (2.26a)$$

To ensure the accuracy of the derivation, the magnitude of $\delta n(x)$ must be much smaller than $N_A(x) + n_{l2}(x)$ instead of $n_{l2}(x)$. So the above equation reduced to

$$-J_n = q D_n(x) \frac{n_{ie}^2(x)}{n_{l2}(x) + N_A(x)} \frac{d}{dx} \left[\frac{[n_{l2}(x) + \delta n(x)][n_{l2}(x) + N_A(x)]}{n_{ie}^2(x)} \right] \quad (2.26b)$$

and solution of which gives,

$$n(x) = \frac{[n_{l2}(0) + \delta n(0)][n_{l2}(0) + N_A(0)] e^{-\frac{\eta \gamma_2 x}{W_b}}}{n_{l2}(x) + N_A(x)} + \frac{[I_1(x) + I_2(x)] e^{-\frac{\eta \gamma_2 x}{W_b}}}{n_{l2}(x) + N_A(x)} \quad (2.27)$$

we express

$$I_1(x) = I_{11}(x) + I_{12}(x) + I_{13}(x) + I_{14}(x) + I_{15}(x) + I_{16}(x)$$

where

$$I_{11}(x) = -\frac{J_n}{q} \left(\frac{a(1-\gamma_2)}{v_s} \right) \left(n(0) - \frac{aJ_{nl2}}{qv_s} - \frac{FW_b}{\eta(1+\gamma_1-\gamma_2)} \right) \left(e^{\frac{\eta x}{W_b}} - 1 \right),$$

$$I_{12}(x) = -\frac{J_n}{q} \left(\frac{a(1-\gamma_2)}{v_s} \right) \left(\frac{aJ_{nl2}}{qv_s \gamma_2} \right) \left(e^{\frac{\eta \gamma_2 x}{W_b}} - 1 \right),$$

$$I_{13}(x) = -\frac{J_n}{q} \left(\frac{a(1-\gamma_2)}{v_s} \right) \left(\frac{FW_b}{\eta(1+\gamma_1-\gamma_2)(\gamma_2-\gamma_1)} \right) \left(e^{\frac{\eta(\gamma_2-\gamma_1)x}{W_b}} - 1 \right),$$

$$I_{14}(x) = -\frac{J_n}{q} \left(\frac{1}{D_n(0)} \left(\frac{N_A(0)}{N_r} \right)^{\gamma_1} \right) \left(n(0) - \frac{aJ_{nl}}{qv_s} - \frac{FW_b}{\eta(1+\gamma_1-\gamma_2)} \right) + \left(\frac{W_b}{\eta(1-\gamma_1)} \right) \left(e^{\frac{\eta(1-\gamma_1)x}{W_b}} - 1 \right),$$

$$I_{15}(x) = -\frac{J_n}{q} \frac{1}{D_n(0)} \left(\frac{N_A(0)}{N_r} \right)^{\gamma_1} \left(\frac{aJ_{nl}}{qv_s} \right) \left(\frac{W_b}{\eta(\gamma_2-\gamma_1)} \right) \left(e^{\frac{\eta(\gamma_2-\gamma_1)x}{W_b}} - 1 \right)$$

$$\text{and } I_{16}(x) = -\frac{J_n}{q} \frac{1}{D_n(0)} \left(\frac{N_A(0)}{N_r} \right)^{\gamma_1} \left(\frac{FW_b}{\eta(1+\gamma_1-\gamma_2)} \right) \left(\frac{W_b}{\eta(\gamma_2-2\gamma_1)} \right) \left(e^{\frac{\eta(\gamma_2-2\gamma_1)x}{W_b}} - 1 \right)$$

we express

$$I_2(x) = I_{21}(x) + I_{22}(x)$$

$$\text{where } I_{21}(x) = -\frac{J_n}{q} \left(\frac{a\eta(1-\gamma_2)}{W_b v_s} \right) N_A(0) \left(-\frac{W_b}{\eta(1-\gamma_2)} \right) \left(e^{-\frac{\eta(1-\gamma_2)x}{W_b}} - 1 \right)$$

$$\text{and } I_{22}(x) = -\frac{J_n}{q} \frac{1}{D_n(0)} \left(\frac{N_A(0)}{N_r} \right)^{\gamma_1} N_A(0) \left(-\frac{W_b}{\eta(1+\gamma_1-\gamma_2)} \right) \left(e^{\frac{\eta(1+\gamma_1-\gamma_2)x}{W_b}} - 1 \right)$$

Assuming that the electron velocity in the base-collector depletion region saturates at v_s , the electron current density J_n at $x = W_b$ is given by

$$J_n = qv_s n(W_b) \quad (2.28)$$

Substituting $x = W_b$ in the expression of $n(x)$ and using (2.28), $n(W_b)$ can be expressed as

$$n(W_b) = n(0)G \quad (2.29)$$

$$\text{The constant } G \text{ is given by } G = \frac{(n_{I2}(0) + N_A(0))e^{-\eta\gamma_2}}{(n_{I2}(W_b) + N_A(0) + (A+B)e^{-\eta\gamma_2})}$$

where

$$A = A_1 + A_2 + A_3 + A_4 + A_5 + A_6.$$

The constants are given as

$$A_1 = v_s \left(\frac{a(1-\gamma_2)}{v_s} \right) \left(n(0) - an_{I2}(W_b) - \frac{FW_b}{\eta(1+\gamma_1-\gamma_2)} \right) (e^\eta - 1),$$

$$A_2 = v_s \left(\frac{a(1-\gamma_2)}{v_s} \right) \left(\frac{an_{I2}(W_b)}{\gamma_2} \right) (e^{\eta\gamma_2} - 1),$$

$$A_3 = v_s \left(\frac{a(1-\gamma_2)}{v_s} \right) \left(\frac{FW_b}{\eta(1+\gamma_1-\gamma_2)(\gamma_2-\gamma_1)} \right) (e^{(\gamma_2-\gamma_1)\eta} - 1),$$

$$A_4 = v_s \left(\frac{1}{D_n(0)} \left(\frac{N_A(0)}{N_r} \right)^{\gamma_1} \right) \left(n(0) - an_{I2}(W_b) - \frac{FW_b}{\eta(1+\gamma_1-\gamma_2)} \right) \left(\frac{W_b}{\eta(1-\gamma_1)} \right) \left(e^{\eta(1-\gamma_1)} - 1 \right),$$

$$A_5 = v_s \left(\frac{1}{D_n(0)} \left(\frac{N_A(0)}{N_r} \right)^{\gamma_1} \right) an_{I2}(W_b) \left(\frac{W_b}{\eta(\gamma_2-\gamma_1)} \right) \left(e^{\eta(\gamma_2-\gamma_1)} - 1 \right)$$

and

$$A_6 = v_s \left(\frac{1}{D_n(0)} \left(\frac{N_A(0)}{N_r} \right)^{\gamma_1} \right) \left(\frac{FW_b}{\eta(1+\gamma_1-\gamma_2)} \right) \left(\frac{W_b}{\eta(\gamma_2-2\gamma_1)} \right) \left(e^{\eta(\gamma_2-2\gamma_1)} - 1 \right)$$

Now

$$B = B_1 + B_2$$

where

$$B_1 = v_s \left(\frac{a\eta(1-\gamma_2)}{W_b v_s} \right) N_A(0) \left(-\frac{W_b}{\eta(1-\gamma_2)} \right) \left(e^{-\eta(1-\gamma_2)} - 1 \right)$$

and

$$B_2 = v_s \left(\frac{1}{D_n(0)} \left(\frac{N_A(0)}{N_r} \right)^{\gamma_1} \right) N_A(0) \left(-\frac{W_b}{\eta(1+\gamma_1-\gamma_2)} \right) \left(e^{-\eta(1+\gamma_1-\gamma_2)} - 1 \right)$$

Substituting the value of $n(W_b)$ in (2.28) we get the expression of J_n as follows

$$J_n = qv_s n(0)G \quad (2.30)$$

The base stored charge per unit area for high injection is

$$Q_n = q \int_0^{W_b} n(x) dx \quad (2.31)$$

The integration in the above charge expression is not easily tractable.

So we have used numerical methods to find the charge.

Using (2.30) and (2.31) the base transit time can be obtained as

$$\tau_b = \frac{Q_n}{J_n} \quad (2.32)$$

2.4 CONCLUSION

In this chapter a mathematical expression for injected electron concentration profile, collector current density and hence base transit time at high level of injection of an exponentially doped *npn* bipolar transistor is obtained considering all the effects especially dependence of mobility on electric field assuming a small change in electron concentration in the base at high injection from its low injection value. The derivation of the model equations starts by first considering low level of minority carrier injection within the base. In the proposed new technique, the minority carrier profile of low level of injection is extended for finding minority carrier profile for high level of injection. The expression of base transit time thus obtained is applicable for all levels of injection. In the next chapter results obtained from the derived equations are plotted and the transit time is compared with that of numerical results available in the literature.

CHAPTER THREE

RESULTS & DISCUSSION

3.1 INTRODUCTION

The mathematical expressions related to this work have been derived in the previous chapter. In this chapter, the analytical equations are calculated to demonstrate the model utility. A computer program is developed based on these derived equations to generate numerical data. Those data are plotted in this chapter to study the effects of various parameters on base transit time.

3.2 RESULTS AND DISCUSSIONS

The transit time through a base with exponential grading of dopant density is modeled and calculated for high level of injection. The results obtained by using the analytical expressions for $n(x)$, J_n , Q_{bn} for high level of injection are analyzed and discussed below. The analytical values have been observed to be in good agreement both with simulation and numeric results.

3.2.1 Distribution of minority carrier within the base

The distributions of minority carrier $n(x)$ within the base for low and high levels of injection for different peak base doping concentrations at different base-emitter voltages are shown in Fig. 3.1(a). The electron concentration profile is not linear due to the built-in electric field caused by the exponential doping concentration. When the peak base doping concentration increases more carriers are injected from emitter to base.

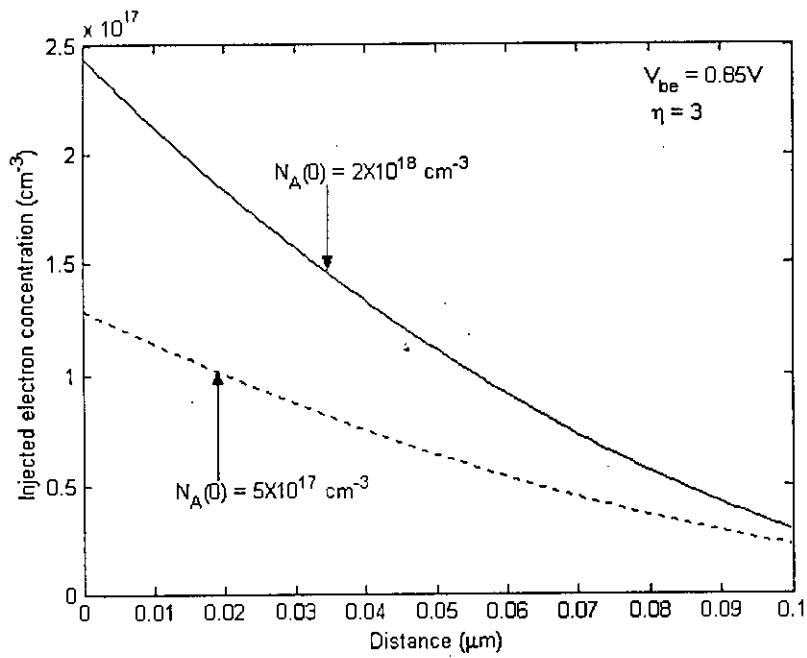


Fig. 3.1 (a) Injected minority carrier distribution within the base for two different peak base doping concentrations.

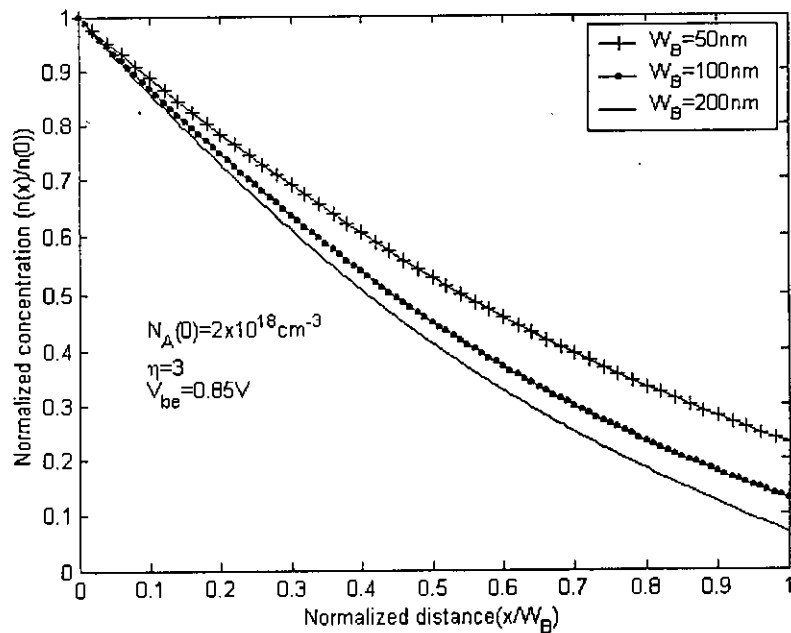


Fig. 3.1(b) Normalized injected electron concentration profile for various base widths.

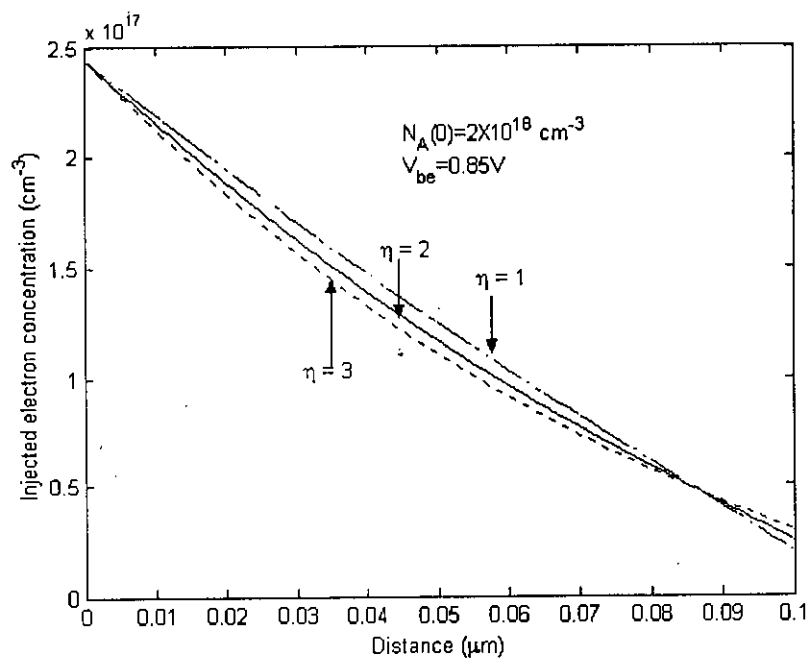


Fig. 3.1(c) Injected minority carrier distribution within the base for various slope of base doping profile.

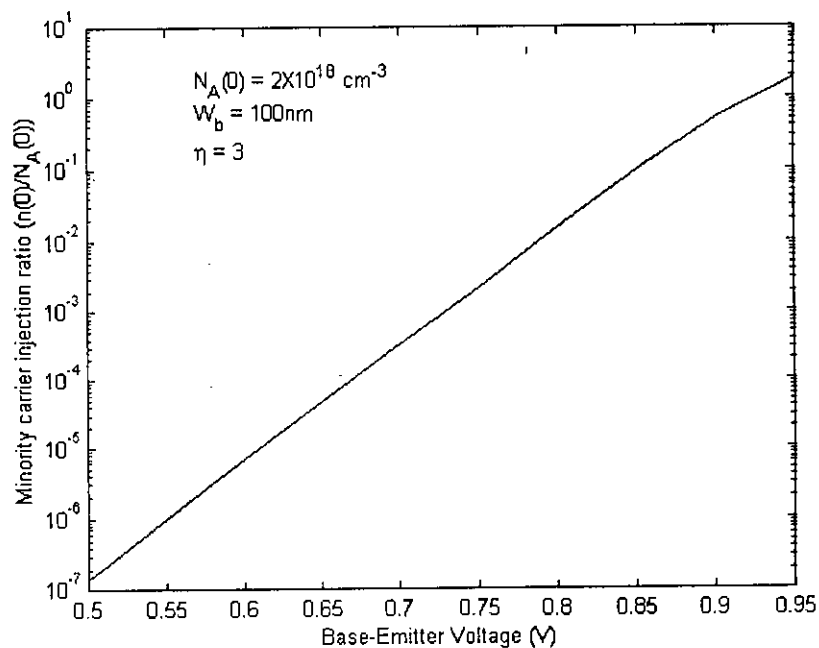


Fig. 3.1(d) Minority carrier injection ratio as a function of base-emitter voltage.

From Fig. 3.1(a), we also see that the minority carrier has maximum value at the emitter-base junction and minimum value at the base-collector junction. In this work, we

consider velocity saturation of electron at the base-collector junction. So at base-collector junction the minority carrier concentrations for low and high levels of injection are not zero.

The dependence of injected electron concentration profile on base-width is shown in Fig. 3.1(b). From this plot, it is clear that, velocity saturation increases the electron concentration more as base width decreases. The electron concentration $n(W_b)$ increases as the base width decreases.

The injected electron concentration profile also depends on the slope of the base doping profile as evident from Fig. 3.1(c). With the increase in the slope of base profile, injected electron concentration decreases more sharply. But velocity saturation increases the electron concentration more as slope of base profile increases.

The variation of minority carrier injection ratio, $n(0)/N_A(0)$ with base-emitter voltage is shown in Fig. 3.1(d). From the Fig. 3.1(d) we see that, the minority carrier injection ratio is an increasing function of base-emitter voltage.

3.2.2 Electric field distribution within the base

Figure 3.2(a) shows the distribution of electric field $E(x)$ within the base for two values of base-emitter voltage and for a given η while Fig. 3.2(b) shows the distribution with varying η . The curves show that, the electric field within the base is negative, i.e., aiding field and constant when base-emitter voltage is low. On the other hand, for high base-emitter voltage it also becomes negative but first its magnitude decreases slowly then increases rapidly near collector-base junction. The equation (2.2) shows that $E(x)$ depends upon both the hole concentration and effective carrier concentration. The quasi-

field due to non-uniform bandgap narrowing is $-\frac{kT\eta\gamma}{qW_b}$. This part of the electric field

is independent of distance from the base-emitter junction. So the variation of electric field with distance is due to the first part of the electric field equation. When the base-emitter voltage is low, $p(x) \approx N_A(x)$ and for exponential base doping the electric field becomes $\frac{kT\eta}{2qW_b}$, which is independent of distance (Fig. 3.2(a)). But $E(x)$ depends upon

η and its magnitude increases with η (Fig. 3.2(b)). Therefore, in the case of low level of

injection electric field is constant within the base region. For high injection, $p(x) = N_A(x) + n(x)$. The change in the aiding field is due to the modulation of electron concentration as well as electron concentration gradient at high injection. For a given η , the magnitude of the aiding field first decreases resulting in total decrease of $E(x)$ and later the aiding field starts increasing with x . This increase causes total increase in magnitude of $E(x)$. Fig. 3.2(a) shows that for a given V_{be} , the magnitude of $E(x)$ decreases with decrease in $N_A(0)$. From the equation of electric field (2.5) we find that with the decrease in $N_A(0)$ the aiding field decreases which results in total decrease in magnitude of $E(x)$. The effect of decrease in $N_A(0)$ in the denominator $2n(x) + N_A(x)$ is dominated by the term $N_A(0)$ in the numerator. Fig. 3.2(a) shows that for a given V_{be} , the magnitude of $E(x)$ increases with increase in η . At high injection with the increase in η the concentration gradient part i.e. aiding field of electric field increases. So this causes the total electric field to increase in magnitude.

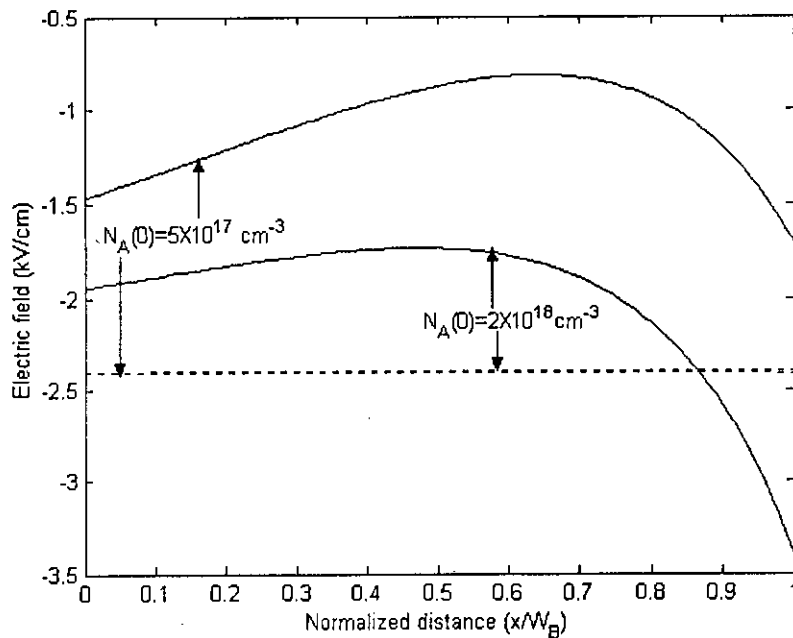


Fig. 3.2(a) Electric field distribution within the base for two different peak base doping concentrations when $\eta = 3$. Solid line represents high injection (for $V_{be} = 0.85\text{V}$) and dotted line represents low injection (for $V_{be} = 0.7\text{V}$).

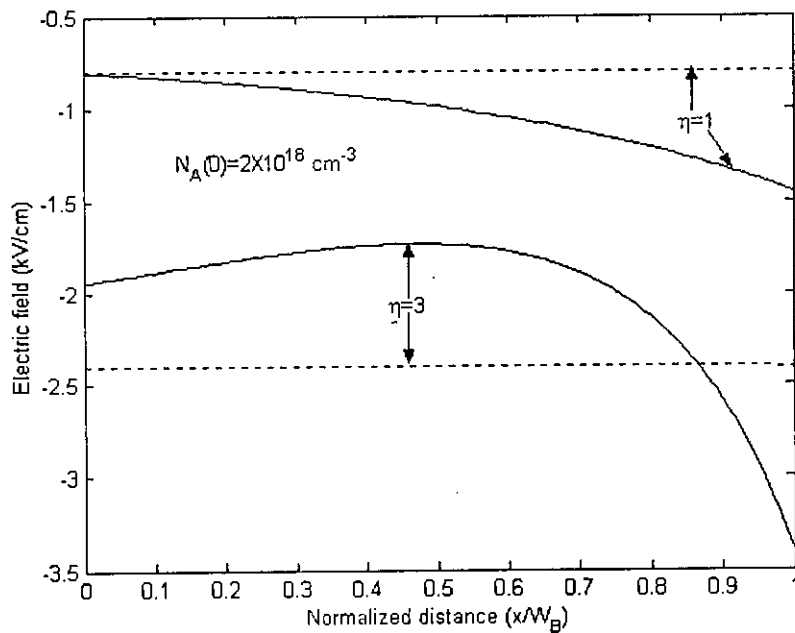


Fig. 3.2(b) Electric field distribution within the base for two different slope of base doping profiles. Solid line represents high injection (for $V_{be} = 0.85\text{V}$) and dotted line represents low injection (for $V_{be} = 0.7\text{V}$).

3.2.3 Variation of collector current density with base-emitter voltage

The variation of collector current density, J_c with base-emitter voltage is shown in Fig. 3.3(a)-(c). From the Fig. 3.1(a)-(c) we see that the collector current density is an increasing function of base-emitter voltage. With the increase in peak base doping concentration, collector current increases at high injection level as evident from Fig. 3.3(a). In Fig. 3.3(b) it is shown that collector current density increases if slope of base doping profile is increased. Finally in Fig. 3.3(c), we justified our current density model by comparing it with the numerical results available in literature [7].

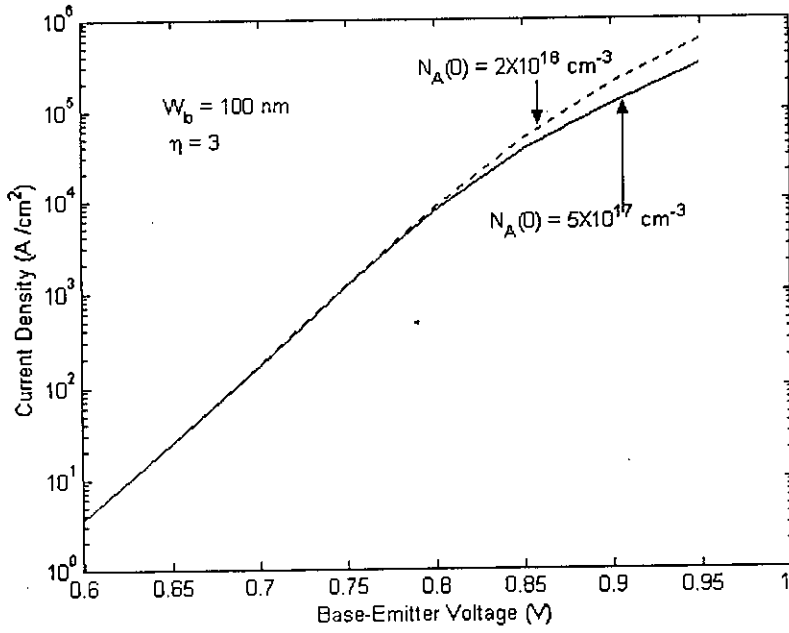


Fig. 3.3(a) Collector current density for two different peak base doping concentrations as a function of base-emitter voltage

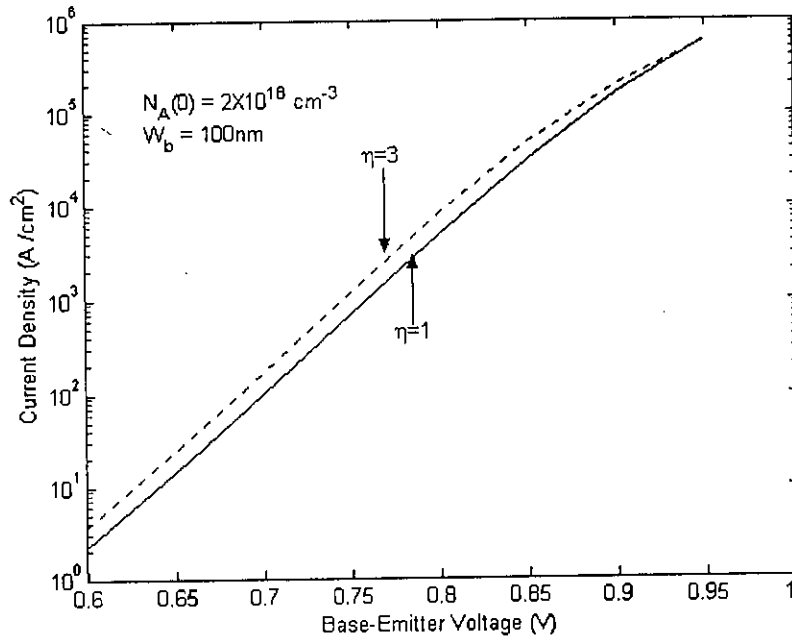


Fig. 3.3(b) Collector current density as a function of base-emitter voltage for two different slope of exponentially doped base.

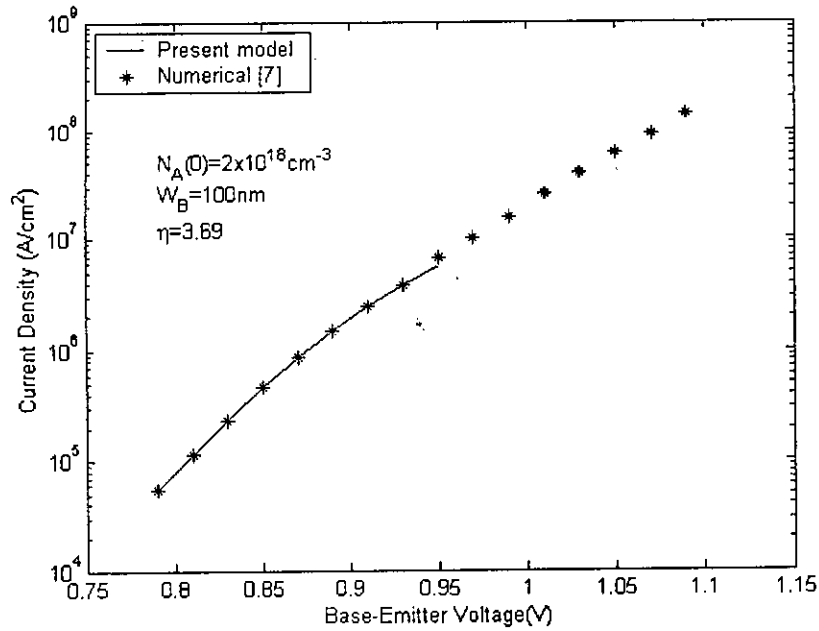


Fig. 3.3(c) Comparison between analytically calculated electron current density and the numeric electron current density [7] as a function of base-emitter voltage.

3.2.4 Variation of base transit time with minority carrier injection ratio

The variations of base transit time, τ_b with minority carrier injection ratio $n(0)/N_A(0)$ for different peak base doping are shown in Fig. 3.4(a). From Fig. 3.4(a) we see that transit time is independent of injection ratio for low level of injection but it is an increasing function of injection ratio at high injection. The value of base transit time is larger for high injection region than that of low injection region. This is due to the reduction of aiding field in the exponentially doped base when the level of injection increases. Due to this effect electrons slow down and hence transit time increases.

In Fig. 3.4(b) the variation of base transit time with minority carrier injection ratio obtained by the present analytical model is compared with the numerical result available in [7]. The two curves show similar variation with minority carrier injection ratio. Results obtained by the proposed model are slightly smaller than that of [7] in high injection region.

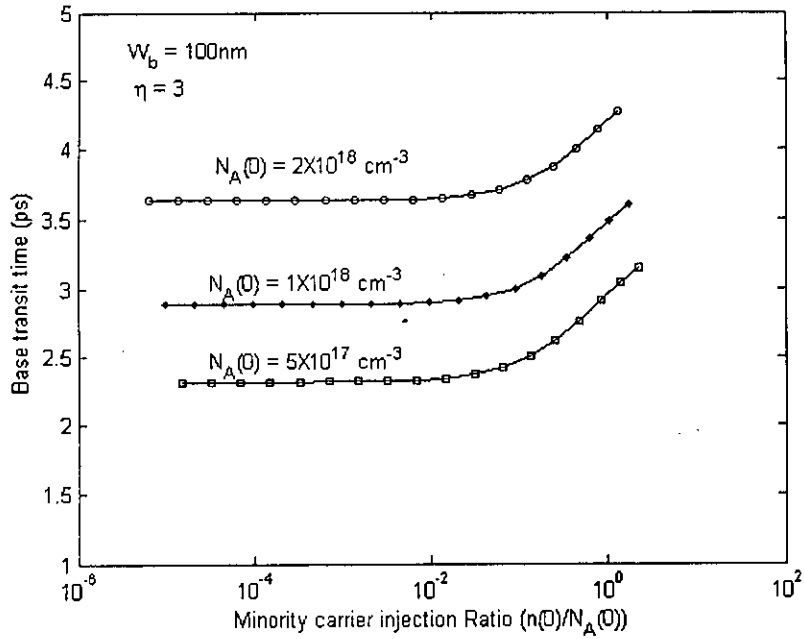


Fig. 3.4(a) Base transit time as a function of minority carrier injection ratio for three different base peak doping concentrations.

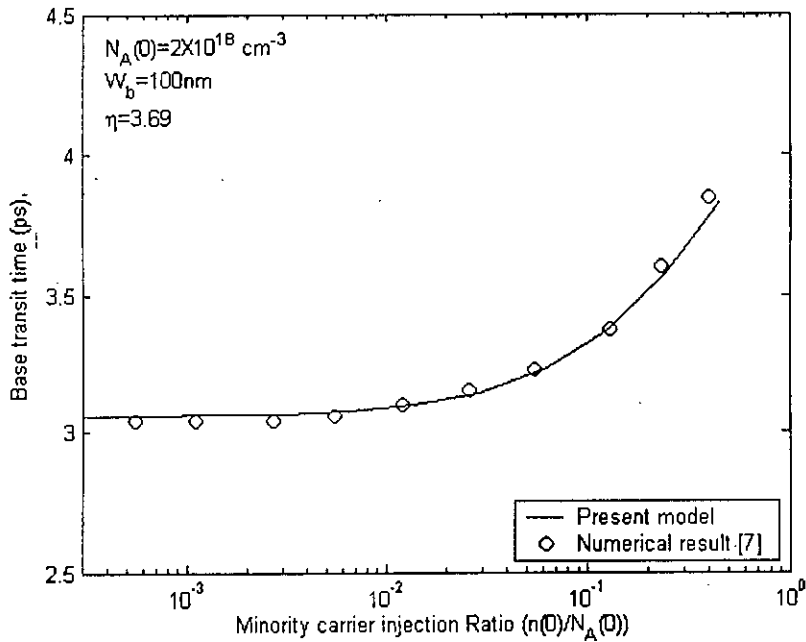


Fig. 3.4(b) Comparison of base transit time as a function of minority carrier injection ratio calculated from the present model with the numerical result [7].

3.2.5 Variation of base transit time with base-emitter voltage

The variation of base transit time with base-emitter voltage for three different peak base doping concentrations is shown in Fig. 3.5. From Fig. 3.5, we see that the variation of base transit time with base-emitter voltage has the same pattern as that with minority carrier injection ratio. As discussed earlier, the minority carrier injection ratio is an increasing function of base-emitter voltage. The increase in base-emitter voltage reduces the aiding field in base and hence the base transit time increases.

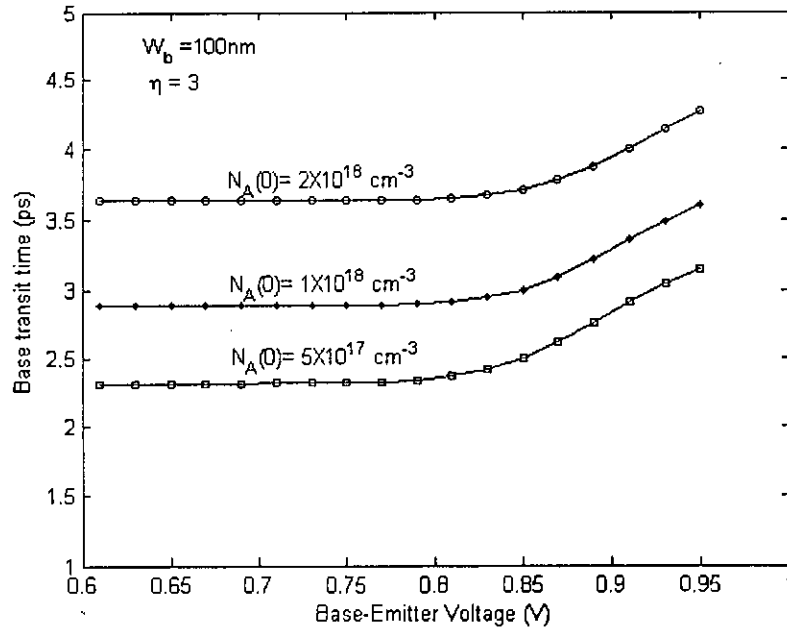


Fig. 3.5 Base transit time for three different peak base doping concentrations as a function of base-emitter voltage.

3.2.6 Dependence of base transit time upon base width

The dependence of base transit time upon base width for various peak base concentrations are shown in Fig. 3.6(a)-(b). From the figures, we see that the base transit time is an increasing function of base width. For the same base width and $N_A(0)$, the base transit time is larger for high level of injection. With the increase of base width the stored base charge increases and electron current density decreases. As base transit time is defined as the ratio of stored base charge to electron current density, base transit time increases with base width. In Fig. 3.6(c) the variation of base transit time with base

width, obtained by the present model is compared with the numerical result available in [20]. The two curves show similar variation of transit time with base width. The two

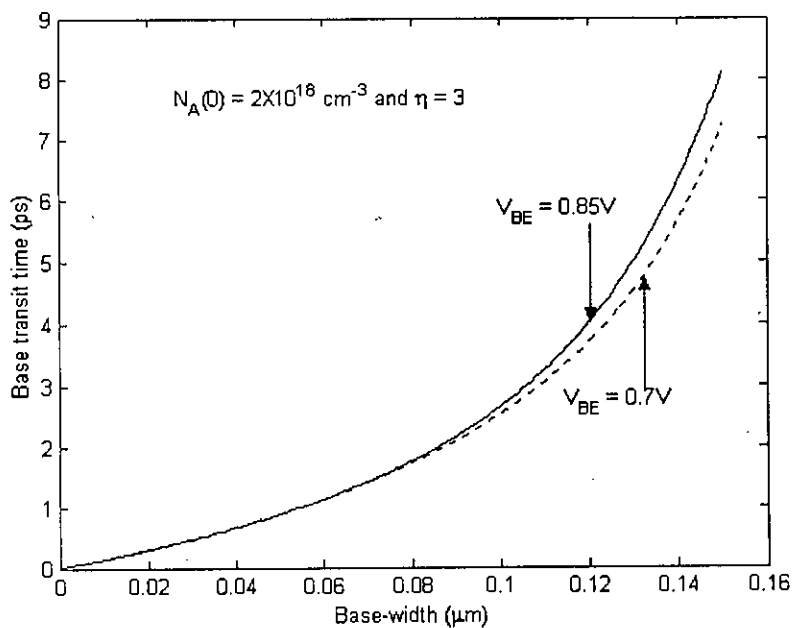


Fig. 3.6(a) Base transit time as a function of base width.

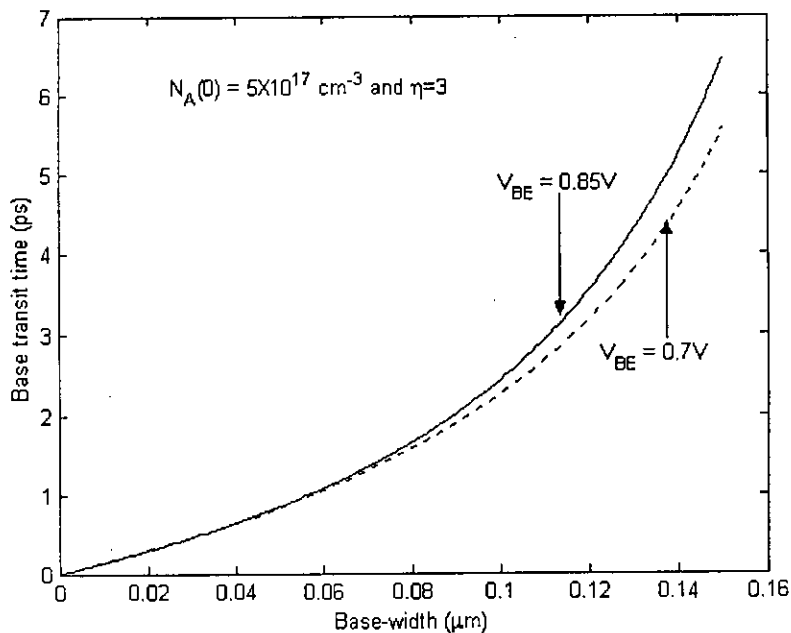


Fig. 3.6(b) Base transit time as a function of base width.

models show almost equal values of base transit time. This supports the validity of the proposed analytical model.

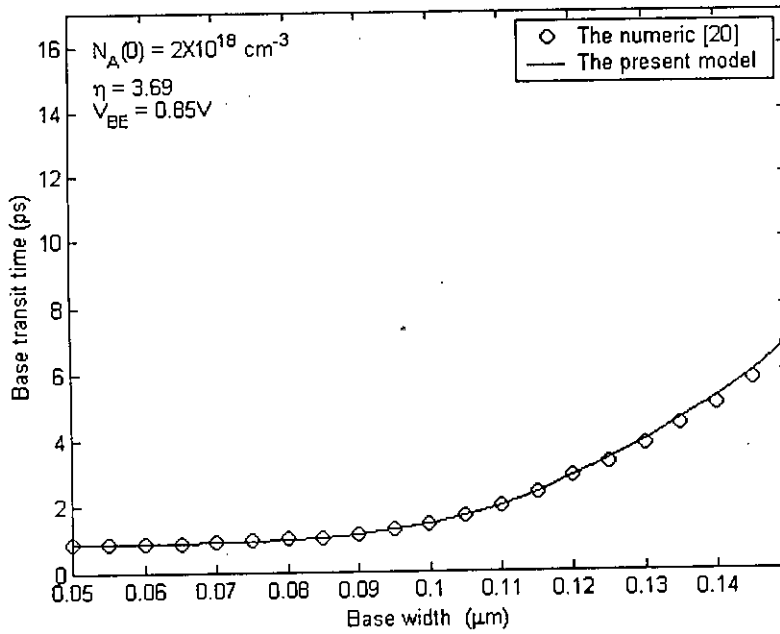


Fig. 3.6(c) Base transit time variation as a function of base width. The circle represents base transit time for [20] and the line represents the present model.

3.2.7 Dependence of base transit time upon peak base doping concentration

The dependence of base transit time upon peak base doping concentration at different base-emitter voltage is shown in Fig. 3.7. From Fig. 3.7, we see that base transit time increases with peak base doping concentration. The dependence of carrier mobility on peak base doping concentration is expressed in Equation (2.6) and (2.7). These expressions show that electron mobility in the base decrease with increase in peak base doping. So base transit time increases with the increase in peak base doping.

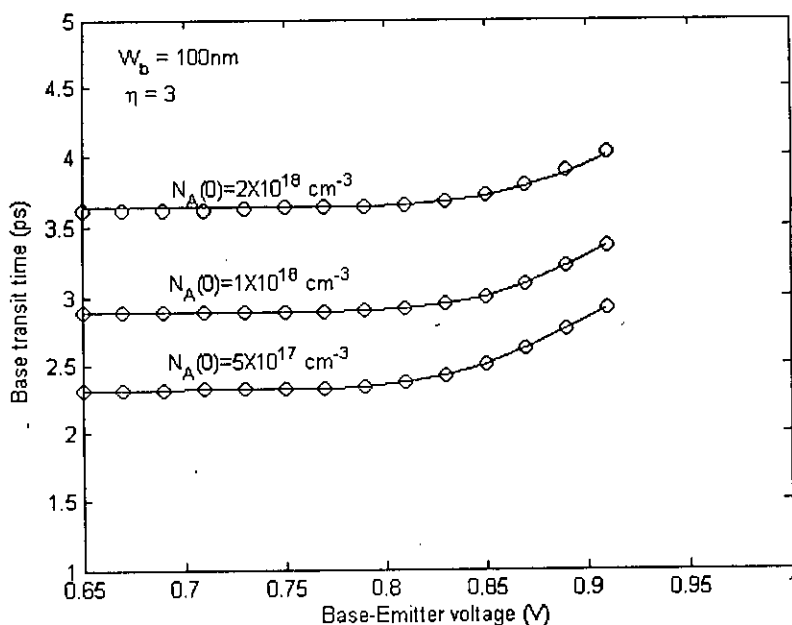


Fig. 3.7 Dependence of base transit time on peak base doping concentration as a function of base-emitter voltage.

3.2.8 Dependence of base transit time upon field dependent mobility

One of the main objectives of this research is to obtain minority carrier profile considering electric field dependence of mobility in addition to doping dependent mobility, bandgap narrowing effect, high-injection effect and carrier velocity saturation. The effect of electric field dependence of mobility on base transit time was investigated and the result is shown in Fig. 3.8. The transit time was found to be higher if the field dependent mobility is considered. This is because minority carrier mobility is inversely related with the electric field. With the increase in electric field minority carrier mobility in the base region decreases. So with the increase in electric field it decelerates the minority carrier transportation through the base region and hence contribute to the increase in base transit time.

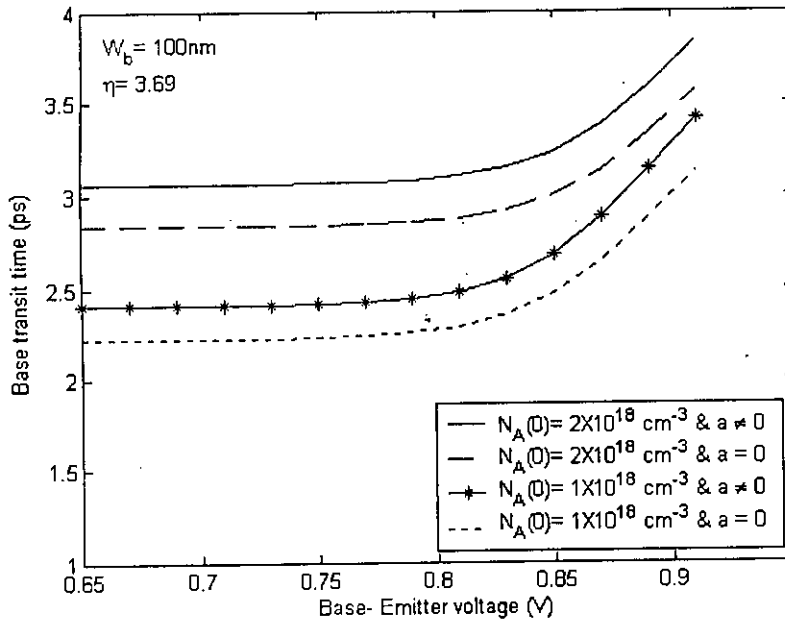


Fig. 3.8 Base transit time as a function of base-emitter voltage with and without considering field dependence of mobility.

3.2.9 Dependence of base transit time upon slope of base doping

The variations of base transit time with the slope of base doping profile for low and high levels of injection are shown in Fig. 3.9. From the Fig. 3.9, we see that the base transit time is a decreasing function of η for both low and high levels of injection. This is because the aiding electric field in the base increases with increase in η . The increase of aiding field will result in total increase in the magnitude of $E(x)$. The increased $E(x)$ will obviously speed up the electron flow and contribute to the lowering of base transit time. From the electric field profile in Fig. 3.2(b) we see that with the increase in η magnitude of electric field increase. So transit time decreases with the increase in the slope of base.

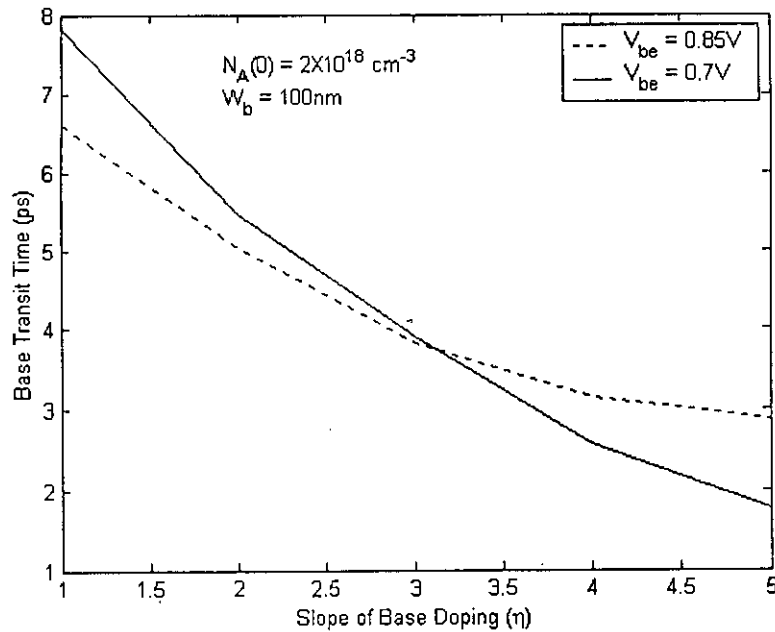


Fig. 3.9 Base transit time as a function of slope of base doping profile.

3.3 CONCLUSION

The analytical expression obtained in chapter two is used to determine the dependence of base transit time on different parameters of BJT such as base-emitter voltage, minority carrier injection ratio, base width, slope of base doping profile and peak base doping concentration. The validity of the approximations made in deriving expressions for $n(x)$, J_n and τ_b are justified by comparing our results with numerical and simulation results. The comparison shows that the proposed analytical expression of base transit time is in good agreement with the available numerical results. The transit time was found to be higher if field dependent mobility is considered.

CHAPTER FOUR

CONCLUSION AND SUGGESTIONS

4.1 CONCLUSION

A base transit time model for an *npn* bipolar junction transistor with exponential-doped base at high level of injection, which is applicable for all levels of injection before the onset of the Kirk effect, is developed. The analytical model is developed assuming a small change in electron concentration in the base of a bipolar junction transistor at high injection from its low injection value. In this work, electric field dependence of mobility in addition to doping dependent mobility, bandgap-narrowing effect, high-injection effect and carrier velocity saturation at the base edge of the base-collector junction are incorporated. The base transit time is found to be different if the field dependent mobility is considered. The study shows that the base transit time depends on base-emitter voltage, minority carrier injection ratio, peak base doping density, slope of base doping profile and base width. The closed form expressions for collector current density minority carrier profile offer a physical insight into device operation and are a useful tool in device design and optimization.

4.2 SUGGESTIONS FOR FUTURE WORK

In this work, the analytical models are applicable for all levels of injection before the onset of the Kirk effect. At the strong high-injection the phenomenon known as Kirk effect will occur. When the Kirk effect occurs the base transit time will become large and will increase with J_C . In future, an expression for transit time considering Kirk effect at strong high injection may be carried out.

REFERENCES

- [1] W. Shockley, "Electrons and Holes in Semiconductors," D. Van Nostrand, Princeton, N.J., 1950, pp. 112.
- [2] J.J. Ebers, "Four-terminal p-n-p-n Transistors," Proc. IRE, 40, 1361 (1952).
- [3] H. M. Rein and M. Moller, "Design consideration for very high-speed Si-bipolar IC's operating to 50Gb/s," *IEEE J. Solid-State Circuits*, vol. 31, pp. 1076-1090, 1996
- [4] J. J. H. van den Biesen, "A simple regional analysis of transit times in bipolar transistors," *Solid-State Electronics*, vol. 29, pp. 529-534, 1986.
- [5] H. Stübing and H. M. Rein, "A compact physical large-signal model for high-speed bipolar transistors at high current densities- Part I: one-dimensional model," *IEEE Trans. Electron Devices*, ED-34, pp. 1741-1751, 1987.
- [6] J. Weng, "A physical model of the transit time in bipolar transistors," *Solid-State Electronics*, vol. 36, pp. 1197-1201, 1993.
- [7] Ma P, Zhang L, Wang Y, "Analytical model of collector current density and base transit time based on iteration method," *Solid-State Electronics*, vol. 39, No. 11, pp 1683-1686, 1996.
- [8] K. Suzuki, "Analytical base transit time model for high-injection regions," *Solid-State Electronics*, vol. 37, pp. 487-493, 1994.
- [9] K. Suzuki, "Analytical base transit time model of uniformly-doped-base bipolar transistors for high-injection regions," *Solid-Sate Electronics*, vol. 36, No. 1, pp. 109-110, 1993.
- [10] M. Pingxi, S. L. Zhang and M. Ostling, "A new set of initial conditions for fast and accurate calculation of base transit time and collector current density in bipolar transistors," *Solid-Sate Electronics*, 2, pp. 2023-2026, 1998.
- [11] Md. Z. R. and M.M.S. Hassan and T.Rahman and A. k. M. Ahsan, "Expression for Base Transit Time in Bipolar Transistors," *Int. J. of Electronics*, vol. 92, No. 4, pp. 215-229, 2005.
- [12] M. M. Shahidul Hassan and A. H. Khondoker, "New Expression for Base Transit Time in a Bipolar Transistor for all levels of Injection," *Microelectronics and Reliability*, vol. 41, No. 1, pp. 137-140, 2001.
- [13] R. S. Muller and T. I. Kamins, "Device electronics for integrated circuits," 1986, 2nd ed. New York: Wiley.
- [14] C. T. Kirk, "A theory of transistor cutoff frequency (f_T) falloff at high current densities," *IRE Trans. Electron. Dev.*, 9, pp. 164-174, 1962.
- [15] W. M. Webster, "On the variation of junction-transistor current-amplifier factor with emitter current," *IRE*, vol. 42, pp. 914-921, 1954.
- [16] J. S. Yuan, "Effect of base profile on the base transit time of bipolar transistor for all levels of injection," *IEEE Trans. Electron. Dev.*, ED- 41, pp. 212-216, 1994.
- [17] K. Suzuki, "Optimum Base-Doping Profile for Minimum Base Transit Time Considering Velocity Saturation at Base-Collector Junction and Dependence of Mobility and Bandgap Narrowing on Doping Concentration," *IEEE Trans. Electron. Dev.*, ED-28, pp. 2102-2107, 2001.
- [18] G. M. Kull, W. Nagel, S. W. Lee, P. Lloyd, E. J. Prendergast and H Dirks, "A unified circuit model for bipolar transistors including quausi-saturation effects,"

- [19] R. J. V. Overstraeten, H. J. Deman and R. P. Martens, "Transport equation in heavy doped silicon," *IEEE Trans. Electron. Dev.*, ED-20, pp. 290-298, 1973. *IEEE Trans. Electron. Dev.*, ED- 32, pp. 1103-1113, 1985.
- [20] M. Pingxi, L. Zhang and Y. Wang, "Analytical relation pertaining to collector current density and base transit time in bipolar transistor," *Solid-State Electronics*, 39, pp. 173-175, 1996.

